The effect of smoke, dust, and pollution aerosol on shallow cloud development over the Atlantic Ocean

Yoram J. Kaufman*†, Ilan Koren*‡, Lorraine A. Remer*, Daniel Rosenfeld§, and Yinon Rudich¶

*National Aeronautics and Space Administration Goddard Space Flight Center, Greenbelt, MD 20771; ‡Joint Center for Earth Systems Technology, University of Maryland, Baltimore County, Baltimore, MD 21228-4664; §Institute of Earth Sciences, Hebrew University of Jerusalem, Jerusalem 91904, Israel; and ¶Department of Environmental Sciences, Weizmann Institute, Rehovot 76100, Israel

Communicated by Veerabhadran Ramanathan, Scripps Institution of Oceanography, La Jolla, CA, June 21, 2005 (received for review January 21, 2005)

Clouds developing in a polluted environment tend to have more numerous but smaller droplets. This property may lead to suppression of precipitation and longer cloud lifetime. Absorption of incoming solar radiation by aerosols, however, can reduce the cloud cover. The net aerosol effect on clouds is currently the largest uncertainty in evaluating climate forcing. Using large statistics of 1-km resolution MODIS (Moderate Resolution Imaging Spectroradiometer) satellite data, we study the aerosol effect on shallow water clouds, separately in four regions of the Atlantic Ocean, for June through August 2002: marine aerosol (30°S–20°S), smoke (20°S–5°N), mineral dust (5°N–25°N), and pollution aerosols (30°N–60°N). All four aerosol types affect the cloud droplet size. We also find that the coverage of shallow clouds increases in all of the cases by 0.2–0.4 from clean to polluted, smoky, or dusty conditions. Covariability analysis with meteorological parameters associates most of this change to aerosol, for each of the four regions and 3 months studied. In our opinion, there is low probability that the net aerosol effect can be explained by coincidental, unresolved, changes in meteorological conditions that also accumulate aerosol, or errors in the data, although further *in situ* measurements and model developments are needed to fully understand the processes. The radiative effect at the top of the atmosphere incurred by the aerosol effect on the shallow clouds and solar radiation is −11 ± 3 W/m² for the 3 months studied; 2/3 of it is due to the aerosol-induced cloud changes, and 1/3 is due to aerosol direct radiative effect.

cloud cover | cloud height | indirect effect | radiative forcing | air quality

During June through August, the Atlantic Ocean is covered by varying concentrations of several aerosol types, each covering a separate latitude belt (see Fig. 1). The Southern Tropical Atlantic (30°S–20°S) is dominated by clean maritime air. The region between 20°S and 5°N is a relatively well defined region covered by smoke from biomass burning in Africa (1, 2). The Northern Tropical Atlantic (5°N–30°N) is under heavy influx of dust from Africa (3), and the Northern Atlantic (30°N–60°N) is impacted by anthropogenic pollution aerosol from North America and Europe. These aerosols absorb and reflect solar radiation to space (4), thereby affecting the regional atmospheric energy balance. Clouds that form in air laden with high aerosol concentrations tend to contain more numerous but smaller droplets that reflect sunlight and cool the Earth (5). The smaller cloud droplets reduce the efficiency of droplet growth by collision coalescence, which at least under some conditions (6) reduce precipitation formation and increase cloud lifetime (7, 8). However, there is a second pathway for aerosols to affect clouds: Smoke, pollution, and dust aerosols absorb solar radiation, heat the atmosphere, and reduce evaporation from the surface (9–11). As a result, smoke over the Amazon or pollution aerosol over the Indian Ocean can inhibit cloud formation (12, 13). This "semidirect effect" (14, 15) was initially predicted to lead to a net global warming effect, but recent studies questioned this conclusion (16, 17). Cloud-resolving models show that absorbing aerosols located above stratiform clouds can strengthen the temperature inversion, thus increasing the moisture and liquid water content of the cloud layer (18). Here we present observations of yet a stronger effect of aerosols on clouds and climate, namely, a substantial increase in shallow cloud coverage due to high aerosol concentrations.

The contradictory pathways by which aerosols can affect clouds, and the large natural variability of cloud properties, represent the largest uncertainty in understanding climate change forcing. A better understanding of the effect requires large-scale systematic measurements to resolve the effect of aerosol on the hydrological cycle and distinguish it from natural variability. Aerosol–cloud interactions over the Atlantic Ocean and in other regions were explored in field experiments (19, 20). In the Atlantic Ocean region, these studies demonstrated connections between aerosol concentration and cloud microphysics. The experiments were intensive in aerosol and cloud physical and chemical characterizations, but were limited in their spatial and temporal extents. Satellite data were used on a global scale to measure the effect of aerosol on cloud droplet size (21, 22) and liquid water content and cloud cover (23). Sekiguchi *et al.* (23) found a 0.10 increase in global cloud cover between pristine and hazy (high aerosol concentration) conditions. However, these studies used satellite data with limited spatial resolution (4–6 km) that cannot resolve smaller clouds, more susceptible to the aerosol effect. They also left open the question of whether the changes in the cloud cover are due to the aerosol effect or to other atmospheric changes that can influence both clouds and aerosol. Here, using the new Moderate Resolution Imaging Spectroradiometer (MODIS)-Terra satellite data of aerosol and clouds with resolution of 1 km, we analyze 3 months (June–August 2002) of data covering millions of km² of shallow (stratiform and trade cumulus) clouds, and the aerosol in their immediate vicinity, and apply multiple regression to distinguish the aerosol impact on clouds from that of coincidentally changing meteorological conditions.

Shallow water clouds have a critical role in the climate system; an increase in shallow cloud cover by only 0.04 is enough to offset 2–3 K of greenhouse warming (24). By reflecting sunlight back to space, stratiform clouds are "the vast *climate refrigerator* of the tropics and subtropics" (ref. 25, see also ref. 26). They are difficult to model because they are only a few hundred meters thick, capped by a strong temperature inversion, and controlled by small-scale physical processes. Using state-of-the-art satellite data, we show that the aerosol concentration is linked to the development, microphysics, and coverage of shallow clouds, thereby generating a large radiative forcing of climate.

Analysis of the Satellite Data

We use the MODIS data on the Terra satellite to measure the daily aerosol column concentration and its correlation to the

Freely available online through the PNAS open access option.

Abbreviations: MODIS, Moderate Resolution Imaging Spectroradiometer; AOT, aerosol optical thickness; LWP, liquid water path; AERONET, Aerosol Robotic Network.

†To whom correspondence should be addressed. E-mail: kaufman@climate.gsfc.nasa.gov.

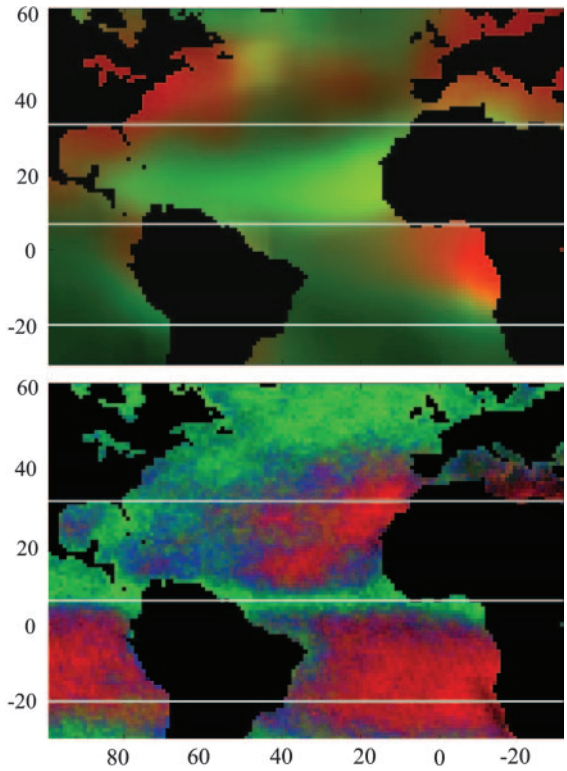

Fig. 1. Spatial distribution of aerosol and clouds over the Atlantic Ocean from Moderate Resolution Imaging Spectroradiometer (MODIS) data for June–August 2002. (*Upper*) Spatial distribution of the aerosol column concentration (expressed as the optical thickness) and type (given by the fraction of the aerosol in the sub-μm mode) over the Atlantic Ocean for the June–August period. The optical thickness is represented by the brightness of the image. The aerosol type is represented by the color: red, dominance by sub-μm particles, smoke from central Africa and pollution from Europe and North America, and green, dominance by dust from Africa or sea salt in regions with high winds. (*Lower*) Spatial distribution of shallow (red), deep convective (green), and mixed (blue) cloud cover on a 1° × 1° longitude × latitude grid. Black indicates continental regions. The data are averaged for June–August 2002.

local stratiform and trade cumulus cloud cover and properties. MODIS observes detailed aerosol and cloud properties with resolution of 0.5–1 km. The data are summarized into a daily 1° × 1° latitude and longitude grid. Simultaneous observations of aerosols in cloud-free regions of the grid box and clouds in the cloudy regions of the grid box are possible (see http://modis-atmos.gsfc.nasa.gov/). Aerosol nonhomogeneity has a spatial scale of 50–400 km (27), allowing the 1° resolution study. MODIS measures the aerosol optical thickness, τ (in cloud-free, sun-glint-free conditions), representing the aerosol column concentration (28), which we use as a surrogate for the concentration of aerosol that interacts with the cloud layer. MODIS also measures the following cloud properties: cloud cover, optical depth, liquid water content, cloud top effective radius, and cloud top pressure (29–31).

The 1° × 1° latitude and longitude data were classified as shallow water clouds if the average cloud top pressure is higher than 640 hPa and all of the clouds in the given grid box and in its surrounding neighboring pixels are water clouds (no ice). The average cloud top pressure of the shallow clouds is 870 hPa, corresponding to 1,200 m. For the region impacted by smoke, 53% of the 1° × 1° grid boxes were classified as shallow clouds (see Table 1). This percentage corresponds to 10^7 km^2 with average of 50 daily observations during the 3 months of investigation. For the region impacted by dust it corresponds to 6×10^6 km^2 of observations (see definition of the studied region in Table 1).

Results

During June through August, smoke, dust and pollution aerosols are confined to separate latitude belts of the Atlantic Ocean (Fig. 1), allowing separate analysis of their effect and the effect of pure marine air on the prevailing clouds (see Table 1). Fig. 2 shows the longitudinal distribution of changes in the shallow cloud cover and in the effective radius (R_{eff}) from clean to aerosol-laden conditions. The fraction of the shallow clouds decreases from east to west because of transition from shallow to convective clouds (see Fig. 1). The largest changes in cloud cover and R_{eff} are observed in regions with high aerosol concentrations near the continental sources. The cloud liquid water path (LWP) increases in all but the biomass-burning zone, in agreement with theory (7). In the smoke zone the LWP decreases.

The satellite data show a systematic increase in the shallow cloud coverage as a function of the aerosol concentration across the Atlantic Ocean for all four aerosol types (see Table 1). For a given value of cloud fraction (0.30), the spatial coverage of shallow clouds extends ≈2,000 km further to the west for heavy smoke or dust in comparison with the clean conditions (Fig. 2).

Table 1. Results of the analysis for four regions in the Atlantic Ocean

Region	Dominant aerosol	Fraction of region	Shallow cloud cover	Range of AOT	Mean AOT	Δ*cl-aer*	δ*cl-aer*	% change in R_{eff}	% change in LWP	Change in CLTP, hPa	Radiative effects (W/m²) due to ΔN_c	ΔN_c + ΔLWP	ΔN_c + ΔLWP + δ*cl*	Total forcing TOA	Δ*Abs*
30°N-60°N	Pollution	0.17	0.07	0.03–0.19	0.102	0.20 ± 0.06	0.19 ± 0.03	−12 ± 10	6 ± 34	−39 ± 20	−1.0	−1.1	−4.5	−8.0	0.7
5°N-30°N	Saharan dust	0.26	0.11	0.03–0.46	0.174	0.36 ± 0.12	0.25 ± 0.04	−12 ± 13	9 ± 34	−66 ± 13	−0.7	−0.9	−6.8	−14.0	0.7
20°S-5°N	Biomass burning	0.53	0.29	0.03–0.43	0.152	0.31 ± 0.07	0.31 ± 0.04	−32 ± 3	−21 ± 8	−55 ± 11	−1.5	−1.0	−9.5	−11.3	2.9
30°S-20°S	Marine	0.47	0.27	0.02–0.24	0.085	0.45 ± 0.10	0.45 ± 0.04	−19 ± 7	35 ± 22	−72 ± 18	—	—	—	—	—

Columns from left: location; dominant aerosol; fraction of the region classified as shallow clouds; shallow cloud fraction; range of the AOT in the analysis (5th, clean, and 95th, hazy percentile), mean value; Δ*cl-aer*, change in the cloud cover from the clean and hazy conditions; δ*cl-aer*, partial change in the cloud cover associated with aerosol by the multiple regression; % change in the cloud effective radius (R_{eff}) from the clean and hazy conditions; % change in the cloud liquid water content (LWP); change in the cloud top pressure (CLTP). For each value the variability among the three months of analysis (June-August) is given. The average radiative effects due to change in the aerosol optical thickness from the base oceanic value of 0.06 associated with the following: increase in cloud droplet concentration (ΔN_c) due to reduction in R_{eff}; + change in the column cloud water content (ΔLWP); + change in the cloud cover (δ*cl*); + direct aerosol radiative effect at the top of the atmosphere (TOA); Δ*Abs*, absorption of sunlight by aerosol. Note that the sum of the last two columns is the total aerosol radiative forcing at the surface. The radiative effect was calculated as half of the effect for solar zenith angle of 60° only for 1° latitude grid boxes characterized as shallow clouds. The uncertainty in the aerosol measurements from MODIS is ≈10%, cloud fraction ≈3%, and cloud effective radius 20%. The 95th percentile confidence limit of the multiple regression is 4–8% off the stated values. The overall error in the radiative effects calculations is therefore ≈20%. Absorption computations depend on the validity of the assumed single scattering albedo with uncertainty of 50%. No calculations are given for the marine region, because the average AOT is too close to the baseline value.

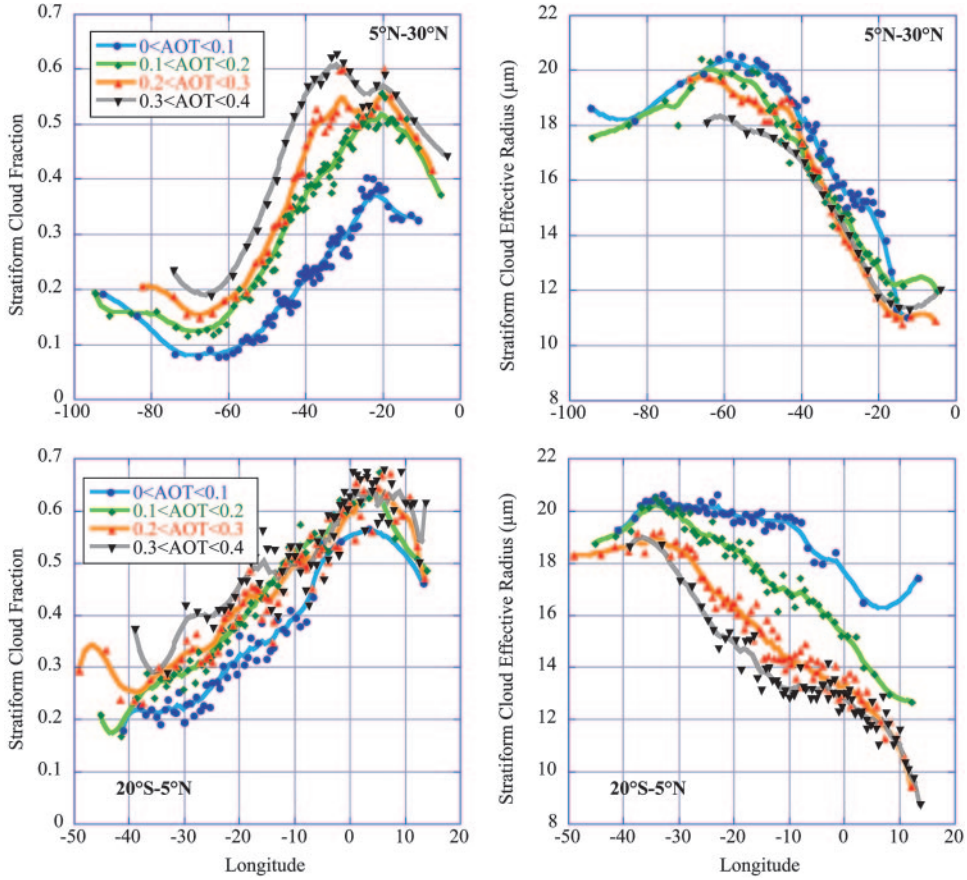

Fig. 2. Longitudinal dependence of the shallow cloud fraction (*Left*) and droplet effective radius (*Right*) for the northern tropical Atlantic with dust intrusions (*Upper*) and southern tropical Atlantic with smoke intrusion (*Lower*). The results are shown for four ranges of the aerosol optical thickness (AOT). The dots are average of 50–200 1° × 1° grid boxes located in similar longitude location and for the same AOT range.

The shallow clouds also form closer to the African coast in smoke-laden conditions. Can the observed changes in the cloud cover be associated with aerosol effects?

Cause and Effect

In Fig. 2 and Table 1 we show the relationship between shallow cloud cover and the presence of aerosols in all four geographical zones analyzed separately for each of the 3 months of this study. Cloud resolving models predict an increase in stratiform cloud cover with an increase in the aerosol concentration (32). However, cloud properties also change because of variation in large-scale atmospheric circulation that may also affect aerosol concentrations. For example, regions of low atmospheric pressures are convergence zones that tend to accumulate aerosol and water vapor and generate conditions favorable for cloud formation (33).

To untangle the effect of aerosol and large-scale meteorology on cloud properties, we use linear multiple regression. Note that the aerosol indirect effect cannot be untangled with high degree of confidence until regional models can predict cloud evolution with high precision. Here we are mainly trying to eliminate the influence of large-scale meteorological parameters that can impact *simultaneously* both aerosol concentration and cloud development, generating false correlation between them. The regression analyzes the dependence of the measured cloud properties (cover, droplet effective radius, and optical thickness) on (*i*) MODIS measurements: aerosol optical thickness (AOT) and total precipitable water vapor (indicator of convergence); and (*ii*) National Center for Environmental Prediction (NCEP)-generated meteorological fields that include air temperature at 1,000 hPa, temperature difference of 850 and 1,000 hPa and 750–1,000 hPa, winds at three altitudes (1,000, 750, and 500 hPa), broad-scale vertical motion at 850 and 500 hPa based on the continuity equation, sea surface temperature, equivalent potential temperature difference between 500 and 950 hPa (34), and low static stability, $(1/\Theta_e)(d\Theta_e/dz)$, where the differential is defined as a finite difference between 850 and 950 hPa. The logarithm of the AOT is used to reduce nonlinearity in the regression. Logarithmic dependence is expected from cloud condensation theory (35), and it was found to be appropriate here. Nonlinearity in the relationships among the parameters may reduce the efficiency of the multiple regression. The analysis is used to address the following questions:

- *What is the sensitivity of the cloud cover to independent variations in meteorological and aerosol parameters?* We find (Table 2) that cloud cover is affected mainly by air temperature at 1,000 hPa, temperature difference 1,000–750 hPa, the AOT, sea surface temperature, and the winds. The influence of aerosol is similar to the influence of these meteorological parameters. This influence of meteorological parameters on MODIS clouds, as expected, shows that the National Center for Environmental Prediction data are relevant to assess simultaneous effects of synoptic meteorological variables on clouds and aerosol.
- *Can changes in the meteorological parameters increase the cloud cover while increasing the aerosol concentration?* We check the systematic change of the meteorological parameters from clean to hazy conditions. The main systematic residual is in the

GEOPHYSICS

Table 2. Multiple regression analysis of the influence of meteorological parameters and dust optical thickness on the cloud fraction analyzed in the 5°N–30°N region of the Atlantic Ocean

Parameter	Correlation to cloud fraction	Correlation to dust AOT	Change in cloud fraction clean to hazy
Temperature at 1,000 hPa	**−0.32 ± 0.09**	**0.22**	**−0.04 ± 0.08**
Temperature difference, 1,000–750 hPa	**−0.31 ± 0.27**	−0.13	**0.05 ± 0.07**
ln(AOT)	**0.29 ± 0.14**	0.97	**0.25 ± 0.03**
Sea surface temperature	**−0.28 ± 0.09**	−0.04	0.00 ± 0.03
Northern wind at 1,000 hPa	**−0.28 ± 0.26**	−0.17	0.01 ± 0.01
Temperature difference, 1,000–850 hPa	**−0.21 ± 0.15**	−0.17	−0.01 ± 0.01
Difference in potential temperature at 500–950 hPa	**0.19 ± 0.07**	−0.06	0.01 ± 0.01
Low static stability at 850 and 950 hPa	−0.17 ± 0.05	0.04	−0.01 ± 0.02
Eastern wind at 1,000 hPa	−0.10 ± 0.08	**−0.20**	0.00 ± 0.01
Northern wind at 750 hPa	−0.09 ± 0.11	0.02	0.00 ± 0.00
Eastern wind at 750 hPa	−0.08 ± 0.07	**−0.24**	**0.06 ± 0.02**
Total column precipitable water vapor	−0.05 ± 0.08	0.20	0.01 ± 0.01
Absolute vorticity at 1,000 hPa	0.04 ± 0.06	−0.14	0.00 ± 0.00
Eastern wind at 500 hPa	−0.02 ± 0.05	**−0.29**	−0.01 ± 0.03

The analysis was carried for 3 months independently, June through August, and the table shows the average and variability among the 3 months. The parameters influencing the cloud fraction are ordered by order of importance based on the correlation with the cloud cover (second column). The next two columns give the correlation of the parameter with the AOT and the change in the cloud fraction associated by the multiple regression with changes in the meteorological parameters or AOT from the 5th to 95th percentile average values. Note that while the AOT is one among seven parameters affecting the cloud fraction, it is by factor five the dominant parameter affecting the change in the cloud fraction from clean (AOT = 0.03) to hazy (AOT = 0.40) conditions. In the smoke, pollution, or marine regions the aerosol effects were even stronger. The main meteorological parameters that affected the difference in the cloud cover from clean to hazy conditions are the air temperature at 1,000 hPa, the difference in the temperature between 1000 and 750 hPa, and the Easterly wind speed at 750 hPa.

dust region (Table 2) by the air temperature difference 1,000–750 hPa and the strength of the Easterly winds at 750 hPa. As a result, the multiple regression suggests that 70% of the change in the cloud cover between clean and dusty conditions is due to the actual dust influence. In the other regions the change in the cloud cover from clean to hazy conditions is similar to the change associated with aerosol (see Table 1).

The associated error in the net aerosol effect within the 95th percentile confidence level, based on the multiple regression, is 4–8% of the effects mentioned. Errors in the meteorological parameters or nonlinearity in the effects could shift some of the dependencies of the cloud cover to aerosol; however, from the multiple regression results we do not expect the errors to be more than double.

Radiative Forcing

Here we compute the radiative impact resulting from the aerosol enhancement of cloud cover, and we compare it with the aerosol indirect radiative effects due to the increase in cloud droplet concentration and LWP. Note that cloud droplet concentration is proportional to (5) $R_{\mathrm{eff}}{}^{-1/3}$ for fixed LWP. Results are summarized in Table 1. The calculations are done in several sequential steps: *Preparatory stage.* The cloud droplet density, LWP, and the cover are all scaled to the baseline clean conditions (36) of AOT = 0.06 from the actual AOT in each grid box of 1° × 1°. The scaling uses the multiple regression-derived dependences of these cloud properties on the AOT. Then, using the M.-D. Chou radiative transfer model (37), we calculate the reflected sunlight at the top of the atmosphere for the clean conditions. *Step 1*. For each grid box of 1° × 1°, we replace R_{eff} and the cloud droplet density from their values for the clean conditions to the actual values, and compute the change in the reflected sunlight (column ΔN_c in Table 1). *Step 2*. We replace the clean condition LWP with the actual value (column ΔN_c + ΔLWP in Table 1). *Step 3*. We replace the cloud cover with the actual value (column ΔN_c + ΔLWP + δcl in Table 1). *Step 4*. We add the direct aerosol effect, assuming that most of the aerosol is above the shallow clouds, because both the dust and the smoke are observed to be at 3-km altitude in this period of the year (1–3). The aerosol properties were taken from the aerosol climatology of Dubovik *et al.* (4). The aerosol effect for the entire study area is shown in Fig. 3.

The results in Table 1 show that the effect of the aerosol-induced change in the cloud cover generates a radiative effect of −3 to −8 W/m^2, or 3–8 times larger than the effect of aerosol-induced changes in the droplet concentration and LWP. The results are comparable to the radiative effects over the Mediterranean Sea derived from field experiment data of −7 W/m^2 at the top of the atmosphere (11). Including aerosol direct effect on solar radiation, the total aerosol radiative effect in the North Atlantic is −8 to −14 W/m^2. This strong radiative effect is not counteracted by the thermal radiative effect due to the low altitude of the clouds. The thermal effect is <0.2 W/m^2.

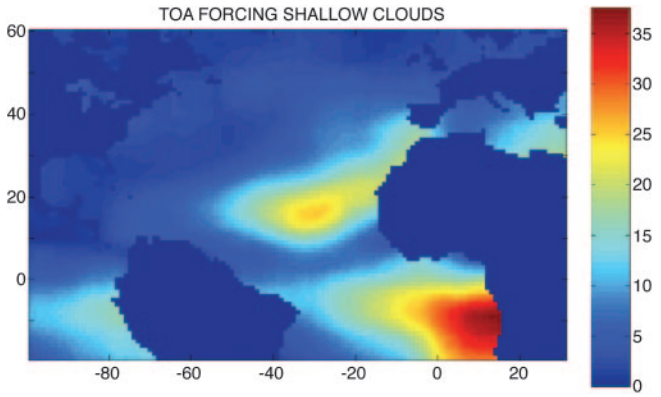

Fig. 3. The aerosol reflected solar flux at the top of the atmosphere due to combined effect on cloud cover and microphysics and on reflection of solar radiation. The radiative effect is calculated as the difference of MODIS observations from the conditions for baseline aerosol with optical thickness of 0.06. The results are weighted by the frequency of detection of shallow clouds in the 1° latitude × longitude daily grid boxes. The color bar shows the values in W/m^2.

The satellite measurements are performed at 10:30 a.m. ± 30 min, local time. However the diurnal cycle of the shallow clouds in this region was shown to be of amplitude of 0.03 in cloud fraction, corresponding to an error in the diurnal average (38) of 7%.

The radiative effect at the surface due to the aerosol and aerosol–cloud interaction is a combination of the radiative effect at the top of the atmosphere + absorption by the aerosol. We estimate the aerosol absorption by using the aerosol climatology of Dubovik *et al.* (4). The results, shown in Table 1, indicate that the surface radiative effect is -9 to -14 W/m^2.

Note that these large radiative effects are found for the season with highest aerosol loading at this region. Myhre *et al.* (G. Myhre, F. Stordall, M. Johnsrud, Y.J.K., D.R., T. K. Bernsten, T. F. Berglen, A. M. Fjærå, and I. S. A. Isaksen, unpublished data) applied similar analysis for the whole globe, and they found a global aerosol indirect forcing of -1.8 W/m^2 through similar processes.

Understanding the Processes

The satellite analysis shows that in all four geographical zones of the Atlantic Ocean, and independently for the 3 months, each with different aerosol properties and meteorology, aerosols systematically increase the shallow cloud cover. In the marine aerosol zone, in the very clean conditions, clouds have difficulties forming. Cloud-resolving models that simulate (32) this condition show an increase in stratiform cloud cover with the increase of aerosol concentration. Aerosols supply the condensation nuclei needed to form cloud droplets. Further increases in aerosol concentrations reduce the size of the droplets and delay or inhibit the formation of precipitation, increasing the cloud cover in the process.

In the smoke-covered zone, the processes are more complex. Further south, Haywood *et al.* (1) observed that the stratiform clouds are detached from the overlaying smoke layer, with a vertical separation of a few hundred meters. A recent modeling study (18) showed that under such conditions the absorption of sunlight by the smoke alone can influence the underlying stratiform clouds even without physical interaction. Solar radiation heats the smoke layer, increasing the strength of the inversion that prevents entrainment of dry air into the stratus clouds below, and thus increases the moisture and the cloud liquid water content in the stratus deck. However, not all of the clouds in this latitude zone are shallow stratiform clouds. Some are trade cumulus clouds that penetrate the smoke layer at 800 hPa. Probably we observe a combination of the increase in cloud cover predicted by Johnson *et al.* (18) and microphysical effects in the trade cumulus as indicated by the strong reduction of the droplet effective radius. Note that we measure the total aerosol column and correlate it with the presence of low shallow clouds. Therefore we can see correlation both in the case of aerosol modifying the cloud microphysics and in the case of aerosol affecting the clouds through modifying the radiation field.

Ackerman *et al.* (40) showed that the inhibition of precipitation is expected to increase entrainment of air from above the clouds. If the air above the cloud is dry the entrainment may reduce the cloud water content. However over the Atlantic Ocean the humid conditions are expected to increase the cloud liquid water content (40), in agreement with our findings.

Data Quality

The satellite analysis of the AOT was evaluated against independent ground-based measurements of the Aerosol Robotic Network (AERONET) sun photometers (41) for ≈30 stations on islands and coastlines around the world (42). This validation, using 2,000 points, shows that the standard error in the satellite optical thickness is $\Delta\tau = \pm 0.03 \pm 0.05\tau$, with a bias of $\Delta\tau \approx 0.008$. The MODIS aerosol cloud screening over the oceans is based on rigorous spatial variability of the reflectances at 0.86 and 1.38 μm (cirrus channel) (43). Can residual cloud contamination still affect the data significantly?

We performed two studies to answer the question (44). In the first we calculated the change in the average aerosol fine fraction (fraction of the optical thickness contributed by fine aerosols) between clear and hazy conditions. Cloud contamination, with its flat spectrum, would have been interpreted by the inversion as coarse aerosols. For smoke or dust the fine fraction increases with the transition from clear oceanic air to high dust or smoke concentrations, contrary to what can be expected because of cloud contamination. For the pollution zone, the fine fraction increases with τ until $\tau \leq 0.3$, and it decreases for higher τ.

In the second study we check whether the AERONET validation with the low bias of $\Delta\tau \approx 0.008$, mentioned above, could have missed cases with cloud contamination or cloud illumination of the aerosol path. In the validation a point is selected if there are at least 2 AERONET measurements during 1 hr around the satellite overpass time and at least 5 ocean measurements of 25 possible in a 50-km zone around the AERONET station. Does this sampling bias the validation to clear skies? We simulated 900 AERONET validations for different cloud conditions to find out. The simulation shows that for an average cloud fraction of 50%, the selected validation data set has an average cloud fraction of only 27%. Therefore, the true cloud contamination and illumination should be roughly twice the contamination observed in the validation data set, or on average doubling the bias to $\Delta\tau \approx 0.016$.

We also studied to what degree cloud detection can be affected by the presence of aerosol. We found it to be independent of the presence of aerosols (45) for aerosol optical thickness $\tau < 0.5$. For $\tau > 0.6$, the aerosol fields affected the cloud classification significantly.

The methodology to derive the cloud droplet effective radius and optical thickness is based on calculations for spatially homogeneous and smooth clouds (30, 31). In reality the cloud bumpiness and inhomogeneities result in overestimation of the effective droplet radius and underestimation of the cloud's optical thickness (46). However, these effects do not depend significantly on the presence of aerosol. Therefore the MODIS retrievals are adequate for studying the correlations between changes in the cloud cover, droplet size, and cloud optical thickness and changes in the surrounding aerosol concentration.

A layer of smoke or dust above the cloud can obscure the cloud properties from the satellite observations. Haywood *et al.* (1, 2) evaluated the cloud retrievals in the presence of African dust and smoke aerosol. They found that the MODIS droplet effective radius (using the 0.86- and the 2.1-μm channels) is not affected by overlying aerosol. We expect the cloud optical thicknesses to be accurately derived (within 10%) in the presence of dust, because dust does not absorb sunlight at 0.86 μm. However smoke can reduce the observed cloud optical thickness by 10–20%.

The point here is to acknowledge several sources of uncertainty in deriving both aerosol and cloud parameters from satellites. However, none of these sources of error can explain the systematically significant relationships we find between aerosol optical thickness and cloud fraction.

Discussion and Conclusions

Three months of daily observations of clouds and aerosol over the Atlantic Ocean show independently that for each month and for each of the four regions, each dominated by a different aerosol type, aerosols have a large effect on the coverage and properties of shallow clouds. The shallow cloud cover increases systematically by 0.20–0.40 with increases in the aerosol column concentration, which is represented by increase in the optical thickness from 0.03 to 0.5. This increase in cloud cover also extends the coverage of shallow clouds thousands of kilometers

west in the smoke- and dust-dominated regions. The changes are accompanied by reduction in cloud droplet size by 10–30%. In most of the regions (all but the smoke region) the liquid water content increases as well. All these observations are in agreement with the suggestion that inhibition of precipitation by aerosol plays a critical role in the formation, cover, spatial extent, and properties of Atlantic shallow clouds. Multiple regression analysis associated most of the increase in the cloud cover with increase in the presence of aerosol and only a small part with changing large-scale meteorological conditions. However, the large-scale and linear nature of the multiple regression analysis leaves uncertainties in the cause and effect that can be resolved with further development of regional cloud-resolving models. The 95th percentile confidence limit on the aerosol effect on cloud fraction is only 4–8% lower than the stated values.

The systematic influence of high aerosol concentrations on clouds generates large radiative effects over the Atlantic Ocean that may regionally counteract the greenhouse warming. Here we can expect that the nonmarine aerosols have doubled in the last 50–100 years, because of expansion of population and economic activity by factor of 3, and a doubling in Saharan dust production (47). The smoke and pollution effect on cloud cover generates a radiative forcing at the top of atmosphere that is about half of today's aerosol effect or -6 W/m^2, and reduction of sunlight available for evaporation from the ocean by 7 W/m^2, thus dominating climate change in this region. This finding is in line with the observation of a global dimming of sunlight at the surface over the land in the last 50 years (48) of 10–20 W/m^2, taking into account the higher aerosol concentrations over the land, near the sources, than over the ocean (1, 49). Recent papers show that the dimming effect reversed in the mid-1980s and a brightening resumed (39, 50). This reversal is also associated with similar reversal in cloud-free transmission of sunlight in Europe and Japan, which is a measure of the aerosol optical thickness. A rough estimate based on figure S4 of Wild *et al.* (39) gives an increase until the mid-1980s and a decrease until 2000 of AOT of 0.01–0.02 per decade, respectively. Scaling the radiative effects in Table 1 to these changes in AOT gives radiative effects of 2–3 W/m^2, in agreement with the measurements (39, 48–50). This agreement suggests that the aerosol indirect effect, and in particular the increase of cloud cover, can serve as a possible explanation for the observed changes in surface illumination.

The forcing observed by aerosol-induced increase in cloud coverage exceeds that due to aerosol-induced changes in cloud drop concentrations alone by a factor of 3–5. These findings clearly demonstrate that traditional estimates of aerosol-cloud forcing, which focused on cloud top brightness, may be inadequate and severely underestimate the aerosol climatic effects.

The aerosol inhibition of precipitation derived indirectly in this study, and the drastic influence, in particular of smoke and dust on the shallow stratiform and trade cumulus clouds, spatial cover, and radiative forcing, leave open the question to what extent these aerosols control the circulation and climate of the Atlantic Ocean. The influence can be expected to be significantly large.

We thank Bruce Wielicki for valuable comments that brought significant improvements in the manuscript. This work was supported by the National Aeronautics and Space Administration, the Israeli Space Agency, and the Israel Science Foundation.

1. Haywood, J. M., Osborne, S. R., Francis, P. N., Keil, A., Formenti, P., Andreae, M. O. & Kaye, P. H. (2003) *J. Geophys. Res.* **108** (D13), 8473, DOI:10.1029/2002JD002226.
2. Haywood, J. M., Osborne, S. R. & Abel, S. J. (2004) *J. R. Meteorol. Soc. A* **130,** 779–800.
3. Prospero, J. M. & Carlson, T. N. (1972) *J. Geophys. Res.* **77,** 5255–5265.
4. Dubovik, O., Holben, B. N., Eck, T. F., Smirnov, A., Kaufman, Y. J., King, M. D., Tanré, D. & Slutsker, I. (2002) *J. Atmos. Sci.* **59,** 590–608.
5. Twomey, S., Piepgrass, M. & Wolfe, T. L. (1984) *Tellus Ser. B* **36,** 356–366.
6. Warner, J. (1968) *J. Appl. Meteorol.* **7,** 247–251.
7. Albrecht, B. A. (1989) *Science* **245,** 1227–1230.
8. Rosenfeld, D. (2000) *Science* **287,** 1793–1796.
9. Ramanathan, V., Crutzen, P. J., Lelieveld, J., Mitra, A. P., Althausen, D., Anderson, J., Andreae, M. O., Cantrell, W., Cass, G. R., Chung, C. E., *et al*. (2001) *J. Geophys. Res.* **106,** 28371–28398.
10. Ramanathan, V., Crutzen, P. J., Kiehl, J. T. & Rosenfeld, D. (2001) *Science* **294,** 2119–2124.
11. Lelieveld, J., Berresheim, H., Borrmann, S., Crutzen, P. J., Dentener, F. J., Fischer, H., Feichter, J., Flatau, P. J., Heland, J., Holzinger, R., *et al*. (2002) *Science* **298,** 794–799.
12. Ackerman, A. S., Toon, O. B., Stevens, D. E., Heymsfield, A. J., Ramanathan, V. & Welton, E. J. (2000) *Science* **288,** 1042–1047.
13. Koren, I., Kaufman, Y. J., Remer, L. A. & Martins, J. V. (2004) *Science* **303,** 1342–1344.
14. Hansen, J., Sato, M. & Ruedy, R. (1997) *J. Geophys. Res.* **102,** 6831–6864.
15. Jacobson, M. Z. (2001) *Nature* **409,** 695–697.
16. Penner, J. E., Zhang, S. Y. & Chuang, C. C. (2003) *J. Geophys. Res.* **108** (D21), 4657, DOI:10.1029/2003JD003409.
17. Lohmann, U. & Feichter, J. (2001) *Geophys. Res. Lett.* **28,** 159–161.
18. Johnson, B. T. (2004) *Q. J. R. Meteorol. Soc.* **130,** 1407–1422.
19. Bates, T. S., Huebert, B. J., Gras, J. L., Griffiths, F. B. & Durkee, P. A. (1998) *J. Geophys. Res.* **103,** 16297–16318.
20. Raes, F., Bates, T., McGovern, F. & Van Liedekerke, M. (2000) *Tellus Ser. B* **52,** 111–125.
21. Nakajima, T., Higurashi, A., Kawamoto, K. & Penner, J. E. (2001) *Geophys. Res. Lett.* **28,** 1171–1174.
22. Bréon, F.-M., Tanré, D. & Generoso, S. (2002) *Science* **295,** 834–838.
23. Sekiguchi, M., Nakajima, T., Suzuki, K., Kawamoto, K., Higurashi, A., Rosenfeld, D., Sano, I. & Mukai, S. (2003) *J. Geophys. Res.* **108** (D22), 4699, DOI:10.1029/2002JD003359.
24. Randall, D. A., Coakley, J., Fairall, C., Kropfli, R. & Lenschow, D. (1984) *Bull. Am. Meteorol. Soc.* **65,** 1290–1301.
25. Bretherton, C. S., Uttal, T., Fairall, C. W., Yuter, S. E., Weller, R. A., Baumgardner, D., Comstock, K., Wood, R. & Raga, G. B. (2004) *Bull. Am. Meteorol. Soc.* **85,** DOI:10.1175/BAMS-85-7-967.
26. Klein, S. A. & Hartmann, D. L. (1993) *J. Climate* **6,** 1587–1606.
27. Anderson, T. L., Charlson, R. J., Winker, D. M., Ogren, J. A. & Holmen, K. (2003) *J. Atmos. Sci.* **60,** 119–136.
28. Tanré, D., Kaufman, Y. J., Herman, M. & Mattoo, S. (1997) *J. Geophys. Res.* **102** (D14), 16971–16988.
29. Ackerman, S. A., Strabala, K. I., Menzel, W. P., Frey, R. A., Moeller, C. C. & Gumley, L. E. (1998) *J. Geophys. Res.* **103,** 32141–32157.
30. King, M. D., Menzel, W. P., Kaufman, Y. J., Tanré, D., Gao, B. C., Platnick, S., Ackerman, S. A., Remer, L. A., Pincus, R. & Hubanks, P. A. (2003) *IEEE Trans. Geosci. Remote Sens.* **41,** 442–458.
31. Platnick, S., King, M. D., Ackerman, S. A., Menzel, W. P., Baum, B. A., Riedi, J. C. & Frey, R. A. (2003) *IEEE Trans. Geosci. Remote Sens.* **41,** 459–473.
32. Ackerman, A. S, Toon, O. B., Stevens, D. E. & Coakley, J. A., Jr. (2003) *Geophys. Res. Lett.* **30** (7), 1381, DOI:10.1029/2002GL016634.
33. Chou, M.-D., Chan, P. K. & Wang, M. H. (2002) *J. Atmos. Sci.* **59,** 748–757.
34. Matsui, T., Masunaga, H., Pielke, R. A., Sr., & Tao, W. (2004) *Geophys. Res. Lett.* **31,** L06109, DOI:10.1029/2003GL019287.
35. Feingold, G., Remer, L. A., Ramaprasad, J. & Kaufman, Y. J. (2001) *J. Geophys. Res.* **106,** 22907–22922.
36. Kaufman, Y. J., Smirnov, A., Holben, B. N. & Dubovik, O. (2001) *Geophys. Res. Lett.* **28,** 3251–3254.
37. Chou, M.-D. (1992) *J. Atmos. Sci.* **49,** 762–772.
38. Rozendaal, M. A., Leovy, C. B. & Klein, S. A. (1995) *J. Climate* **8,** 1795–1809.
39. Wild, M., Gilgen, H., Roesch, A., Ohmura, A., Long, C. N., Dutton, E. G., Forgan, B., Kallis, A., Russak, V. & Tsvetkov, A. (2005) *Science* **308,** 847–850.
40. Ackerman, A. S., Kirkpatrick, M. P., Stevens, D. E. & Toon, O. B. (2004) *Nature* **432,** 1014–1017.
41. Holben, B. N., Eck, T. F., Slutsker, I., Tanré, D., Buis, J. P., Setzer, A., Vermote, E., Reagan, J. A., Kaufman, Y. J., Nakajima, T., *et al.* (1998) *Remote Sens. Environ.* **66,** 1–16.
42. Remer, L. A., Tanré, D., Kaufman, Y. J., Ichoku, C., Mattoo, S., Levy, R., Chu, D. A., Holben, B., Dubovik, O., Smirnov, A., *et al*. (2002) *Geophys. Res. Lett.* **29** (12), 1618, DOI:10.1029/2001GL013204.
43. Martins, J. V., Tanré, D., Remer, L. A., Kaufman, Y., Mattoo, S. & Levy, R. (2002) *Geophys. Res. Lett.* **29** (12), 8009, DOI:10.1029/2001GL013252.
44. Kaufman, Y. J., Remer, L. A., Tanré, D., Li, R., Kleidman, R., Mattoo, S., Levy, R., Eck, T., Holben, B. N., Ichoku, C. *et al*., *IEEE TGRS*, in press.
45. Brennan, J. I., Kaufman, Y. J., Koren, I. & Li, R. R. (2005) *IEEE TGRS* **43,** 911–915.
46. Várnai, T. & Marshak, A. (2002) *J. Atmos. Sci.* **59,** 1607–1618.
47. Prospero, J. M. & Lamb, P. J. (2003) *Science* **302,** 1024–1027.
48. Stanhill, G. & Cohen, S. (2001) *Agric. Forest Meteorol.* **107,** 255–278.
49. Ichoku, C., Remer, L. A., Kaufman, Y. J., Levy, R., Chu, D. A., Tanré, D. & Holben, B. N. (2003) *J. Geophys. Res.* **108** (D13), 8499, DOI:10.1029/2002JD002366.
50. Pinker, R. T., Zhang, B. & Dutton, E. G. (2005) *Science* **308,** 850–854.